

AN ALTERNATIVE VIEW OF FLAT ROTATION CURVES. II. THE OBSERVATIONS

D.S.L. Soares

Observatório Astronômico da Piedade
 Departamento de Física, ICEx, UFMG, Brazil

Received 1993 July 26

RESUMEN

Se investigan las curvas de rotación de 20 galaxias espirales usando el modelo propuesto por Soares (1992) que tiene como característica principal la de atribuir una alta razón M/L ($= 30$; $H_0 = 50 \text{ km s}^{-1} \text{ Mpc}^{-1}$) para la materia visible. La rotación observada de todas las galaxias puede ser ajustada sin hacer la suposición de un halo oscuro.

Sin embargo, se sugiere que el hecho de que casi todas las medidas disponibles de velocidades de rotación son deducidas a partir de líneas emitidas por el gas de las galaxias (neutro o ionizado) las hace inadecuadas como indicadores del potencial gravitacional. Para considerar esto, el modelo introduce un potencial efectivo apropiado para describir la hidrodinámica dentro del disco gaseoso. La morfología general de las curvas [i.e., la presencia de una meseta en $V(r) \times r$] se interpreta, en este tratamiento, como una consecuencia de las características hidrodinámicas de los discos galácticos.

La relación de Tully-Fisher se expresa en términos de los parámetros del modelo y se usa como una restricción adicional en el proceso de ajuste del modelo a la rotación observada de las galaxias.

ABSTRACT

The rotation curves of 20 spiral galaxies are examined in the light of a toy model (Soares 1992) which has as the main feature the assignment of a high M/L ratio ($= 30$; $H_0 = 50 \text{ km s}^{-1} \text{ Mpc}^{-1}$) to the visible matter. The observed rotation of all galaxies can be accommodated without the assumption of a dark halo.

Moreover, the suggestion is made that the fact that almost all available rotational velocity measurements are derived from emission lines emitted by gas in galaxies (either neutral or ionized) makes them inappropriate as tracers of the galaxy gravitational potential. To account for that, the model introduces an effective potential meant to describe the hydrodynamics inside a gaseous disk. The general morphology of the curves [i.e., the presence of a plateau in $V(r) \times r$] is interpreted in this framework as a consequence of the hydrodynamical characteristics of disks in galaxies.

The Tully-Fisher relation is expressed in terms of model parameters and used as an additional constraint in the process of fitting the model to the observed rotation of the galaxies.

Key Words: GALAXIES—SPIRAL — GALAXIES—KINEMATICS AND DYNAMICS

1. INTRODUCTION

The mass discrepancy in spiral galaxies is still an unsolved problem in astrophysics. Topical or review papers have been copiously written in the last decade (e.g., Faber & Gallagher 1979; Rubin et al. 1982; Whitmore et al. 1984; van Albada et al. 1985; van Albada & Sancisi 1986; Trimble 1987; Sanders 1990; Broeils 1992; Ashman 1992; Persic & Salucci 1993) demonstrating renewed interest on the subject.

The orthodox explanation of flat rotation curves of spiral galaxies is that they are the result of combined effects of luminous matter, with M/L typical of the solar neighborhood, and dark matter with much higher M/L . Luminous matter accounts for the rotation inside the luminous body and a dark extended halo is needed to fully account for the values above Keplerian observed in the outer regions of spirals. Popular alternative views include modifications of Newtonian dynamics (or gravity,

e.g., Milgrom 1983, 1988, 1991), and modifications of the classical view of spiral galaxies (e.g., Valentijn 1990; González-Serrano & Valentijn 1991; Battaner et al. 1992). This paper follows another (Soares 1992, hereafter Paper I) where we put forward an alternative idea for the mass discrepancy query.

In Paper I we suggested that real M/L for the luminous body of spiral galaxies should be those obtained from binary galaxy studies (e.g., Schweizer 1987; Soares 1989), which are as large as ten or fifteen times the local solar M/L . These values, in spite of disagreeing with classical stellar population calculations (e.g., Larson & Tinsley 1978), are by no means ruled out by standard stellar population synthesis of spiral galaxies; it is almost common sense nowadays that a population synthesis calculation of spiral galaxies can yield virtually any value of M/L , given the uncertainty on stellar metallicities and ages.

Furthermore, we pointed out that the observations of the rotation of spiral galaxies are inferred almost always from Doppler shifts of emission lines generated either by ionized or by neutral gas in galaxies, and gas motion cannot be used as a reliable tracer of the gravitational potential. Rather, gas motion is ruled by an *effective* potential wherein hydrodynamical effects are incorporated.

The last two paragraphs state the two basic work hypotheses of the alternative model (hereafter AMOD) described in Paper I.

In § 2 a short summary of the toy model of Paper I is made. The rotation curves of 20 spiral galaxies, observed by Rubin et al. (1982) are investigated in the framework of the AMOD potential (see eq. [1], below). In order to reduce the number of free parameters, we assume a fixed M/L for all of the galaxies in our sample. The adopted value is $M/L = 30$ (for $H_0 = 50 \text{ km s}^{-1} \text{ Mpc}^{-1}$, here and throughout this paper). This figure is consistent with binary galaxy studies and is further justified by the application of the toy model to the well-known spiral galaxy NGC 3198 (e.g., van Albada et al. 1985; Begeman 1987, 1989); this is done in § 3. In § 4, an expression for the Tully-Fisher relation (Tully & Fisher 1977), in terms of model parameters, is derived, the fitting process is described and applied to the sample. The resulting Tully-Fisher diagram is plotted as well. A brief discussion of the results and our final conclusions are presented in § 5.

2. AMOD

The overall kinematics of gas in spiral galaxy disks is derived from the toy potential

$$U(r) = \frac{GM}{r} \left(1 + \beta e^{-r/r_0} \right), \quad (1)$$

where β and r_0 are intrinsic scale parameters in galaxies.

A Seeliger-Neumann type potential (North 1961; Assis 1992) was added to the Newtonian gravitational potential in order to describe the hydrodynamics inside a spiral gaseous disk; the parameters β and r_0 determine the range of applicability of the new potential component in each galaxy. In Paper I, this additional component is associated with a kind of *buoyancy* potential. It is shown there also that equation (1) can be derived from a simple phenomenological description of the dynamics of gas bubbles inside smooth gaseous disks.

The circular velocity of test particles is easily derived from the AMOD potential:

$$v_{\text{circ}}(r) = \left\{ \frac{GM}{r} \left[1 + \beta \left(1 + \frac{r}{r_0} \right) e^{-r/r_0} \right] \right\}^{1/2}. \quad (2)$$

The Keplerian rotation curve derived from the light profile of a spiral galaxy plus the usual values of M/L is below observed gas rotation in the outer regions. The conventional dark matter approach is to adopt an extended halo in such a way that the model velocities are pushed up to the observed levels. AMOD, on the other hand, assumes higher M/L , resulting in that the Keplerian curve will be located above the observed rotation curve. With properly chosen β and r_0 it was shown in Paper I that equation (2) pulls down such an overestimated rotation profile to the observed levels. This is illustrated in Figure 1, where we plot the rotation curve of a conventional $M/L = 30$ spiral galaxy. The Keplerian circular velocities are below the observations and are reconciled with them with the aid of a dark halo. Also shown

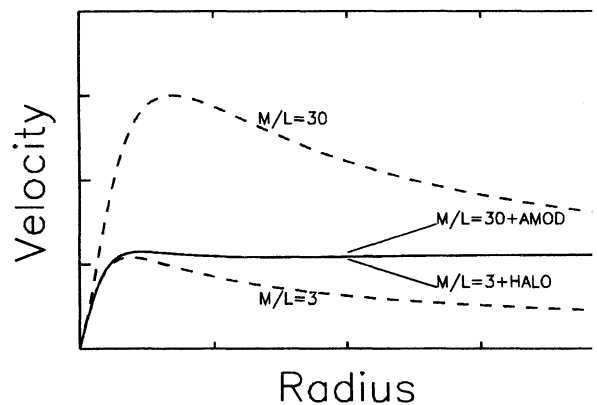


Fig. 1. A typical flat rotation curve can be explained by a summing galaxy luminous matter with solar neighborhood M/L plus a dark halo. Alternatively, it can also be explained with luminous matter having a high M/L at test particle circular velocities given by AMOD.

the Keplerian rotation curve of a $M/L = 30$ spiral galaxy that does not fit the observations as well. In this latter case the AMOD potential is applied and the observations are now well fitted. The exponential decay component present in the AMOD potential represents an additional repulsive force of hydrodynamical origin, which acts on the test particles that are tracing the galaxy rotation.

3. AMOD FIT TO NGC 3198

As we have pointed out in Paper I, AMOD has the same mathematical formulation as the model suggested by Sanders (1984, 1986) to account for mass discrepancies in spiral galaxies, i.e., both are described by the same potential given by equation (1) with the sole difference that, in Sanders' model, the gravitational constant G is replaced by a new G_∞ (see below). This model, named FLAG (*finite length-scale anti-gravity*), was later abandoned by Sanders (1990), among others, mainly on the grounds of its inability to explain one of the most important observed features of spiral galaxies, namely the Tully-Fisher relation.

In FLAG, due to the new potential component (the very same Seeliger-Neumann potential shown above) the "effective" gravitational constant is now $G_\infty = G/(1+\beta)$, where β , in the context of FLAG, is the coupling constant of the additional component of gravity¹. G is the usual Newtonian gravitational constant. Sanders has used the galaxy NGC 3198 to find out what are the values of FLAG's universal constants, r_0 and β . He found, for a luminous disk with $M/L = 2.4$, $r_0 = 36$ kpc and $\beta = 0.92$ (for $H_0 = 50$ km s⁻¹ Mpc⁻¹). These values can be used to calculate the AMOD M/L of NGC 3198, i.e., $2.4/(1+\beta) = 30$. They are also used to fit the observed rotation curve of NGC 3198 with equation (2). Again, as in Paper I, we represent M by a Plummer sphere (an $n = 5$ polytrope). Its cumulative mass distribution is given by

$$M(r) = \frac{M_o r^3}{(r^2 + \epsilon^2)^{3/2}}, \quad (3)$$

where M_o is the total galaxy mass and ϵ is the Plummer sphere core radius. In order to account for the fact that spirals have constant central surface brightness of $\approx 140 L_\odot \text{ pc}^{-2}$ (Freeman 1970; Schweizer 1976), the core radius is scaled to the total galaxy mass as (e.g., Sanders 1988):

$$\epsilon = 1.6 M_o^{1/2}. \quad (4)$$

M_o is given in units of $10^{11} M_\odot$ and ϵ in kpc. The total luminosity (B band) of NGC 3198 is $2.0 \times 10^{10} L_{B\odot}$ (Begeman 1987), which implies $M_o = 6.0 \times 10^{11} M_\odot$ and $\epsilon = 3.9$ kpc. Equation (4) is also used below (in § 4) to model all the sample galaxies.

Figure 2 shows the fit to the observed rotation curve of NGC 3198 obtained with the above-mentioned parameters. The only difference between the AMOD fit and FLAG's one is the use by Sanders of an exponential disk to model the galaxy. It can be seen that with the spherical symmetric Plummer model the fit does not change too much. The general behavior of the rotation curve is reproduced in spite of losing fine features.

From the above investigation on NGC 3198, and from results of binary galaxy studies (e.g., Schweizer 1987; Soares 1989), we shall adopt the value of $M/L = 30$ to proceed with the AMOD analysis. Of course, the M/L of a given galaxy is an intrinsic parameter and might vary from galaxy to galaxy. The point here is that fixing M/L , we gain in reducing the free parameter space while not being too far from what ought to be individual values of M/L for each galaxy. It is worthwhile noting that, in the context of AMOD, such a high M/L is assigned to the *visible* body of the galaxy instead of being justified by the artificial assumption of the existence of an extended dark halo surrounding the visible galaxy.

The sample of 20 Sb galaxies of Rubin et al. (1982) will be considered in the next section taking into account the AMOD potential and the Tully-Fisher relation.

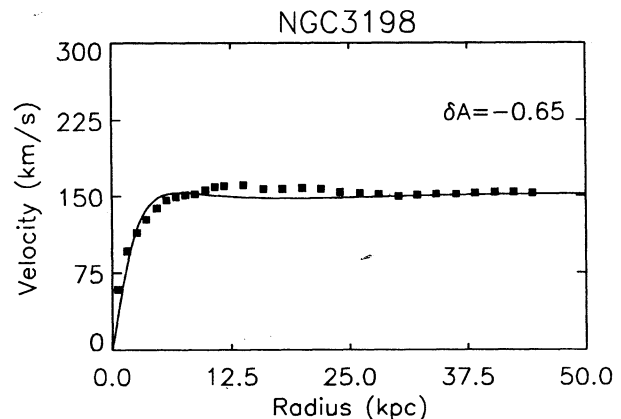


Fig. 2. The filled squares are the observed H I circular velocities for NGC 3198 (Begeman 1987). The solid line is the AMOD fit to the observations with $\beta = -0.92$, $r_0 = 36$ kpc, and $M/L = 30$. The galaxy mass distribution is modeled with a Plummer model.

¹ It is important to stress that in AMOD such a component is not an additional component of gravity, rather, it is a part of the "effective" potential in galaxies, and is responsible for describing the hydrodynamical behavior of gas test particles inside a gaseous disk.

4. AMOD AND THE TULLY-FISHER RELATION

The main question in this section is whether AMOD is consistent or not with the Tully-Fisher relation. To investigate that, a set of observed rotational profiles is modeled with AMOD having the Tully-Fisher relation as an additional fitting constraint.

To begin with, one needs a convenient expression for the Tully-Fisher relation, i.e., a relationship which involves the relevant AMOD parameters. Let us consider the following form of the Tully-Fisher relation (Aaronson, Huchra, & Mould 1979):

$$L = k_{TF} V_p^4, \quad (5)$$

which, in spite of being oversimplified, is very useful to the sort of investigation underway.

For the evaluation of k_{TF} we have considered the spiral galaxies observed in the 21-cm line of neutral hydrogen by Begeman (1987). We took, for Begeman's eight galaxies, the luminosity in the B band (L) and the plateau velocity of the rotation curve (V_p). From a plot of $L \times V_p^4$, and in a system of units where luminosity is given in $10^{11} L_\odot$, time in 10^8 s, velocity in units of 97.8 km s^{-1} and $G = 4.50$, we derive $k_{TF} = 2.87 \times 10^{-2}$. A range of 30% error is allowed in equation (5) (see below) to account for the scattering in the diagram $L \times V_p^4$ which was used for the determination of k_{TF} .

The AMOD parameters are introduced in equation (5) through the expression for the circular velocity given by equation (2). Let $V_p = v_{circ}(r = 2 \times R_{25})$, where R_{25} is the de Vaucouleurs' radius of the galaxy (i.e., the radius of the galaxy to the 25th B magnitude per square arcsecond isophote). This is an arbitrary value for the model plateau velocity but the particular choice of V_p (at some $r \geq R_{25}$) does not change the analysis, as we have verified. The galaxy mass is converted into integrated blue luminosity via the M/L ratio. We can then re-write equation (5) as

$$A = \frac{1}{G k_{TF} V_p^2}, \quad (6)$$

where A is the AMOD index, and is given by:

$$A = \frac{M/L}{2R_{25}} \left[1 + \beta \left(1 + \frac{2R_{25}}{r_o} \right) e^{-2R_{25}/r_o} \right]. \quad (7)$$

The Tully-Fisher relation is now expressed through a relationship between the so-called AMOD index A and V_p (eq. [6]). $A(V_p)$ is the AMOD function one would expect if the Tully-Fisher relation can be expressed as equation (5). Equation (7) can be used then to derive an *observed* AMOD index (A_{fit}),

taking into account intrinsic parameters of the galaxies (β , r_o , R_{25} and M/L). The AMOD parameter β and r_o , are obtained from the fits to the rotation curves.

A fit of the AMOD circular velocity to Rubin et al. (1982) observations of the rotation of 20 Sb spiral galaxies was done. The fitting procedure took into account the goodness of fitting to the Tully-Fisher relation (eq. [6]) too. A quantitative measure of the fitting of A_{fit} (defined through eq. [7]) to equation (6) can be given by δA , defined by

$$\delta A = \frac{A(V_p) - A_{fit}}{0.30A(V_p)}. \quad (8)$$

This quantity gives the amount of deviation of the fitted AMOD index from the predicted $A(V_p)$ curve in terms of a 30% error bar. The AMOD solution: $V_{AMOD}(r)$, for the rotation curves measured by Rubin et al., $V_{obs}(r)$, are those that simultaneously minimize $|\delta A|$ and $\Delta V = |V_{obs}(r) - V_{AMOD}(r)|$.

Figure 3 and Figure 4 show the result of the fitting process. The observed rotation curves by Rubin et al. are shown together with the AMOD fit in Figure 3. The Tully-Fisher relation is shown in Figure 4. Table 1 presents the relevant parameters of all studied galaxies. Column 1: galaxy name (NGC or UGC); column 2: plateau velocity, as given by Rubin et al. and by Begeman in the case of NGC 3198; column 3: de Vaucouleurs' radius, in kpc; column 4: characteristic AMOD radius, in kpc; column 5: AMOD coefficient β ; column 6: AMOD index, defined by equation (7); column 8: relative error in A , defined by equation (8).

Both trends, in the rotational profiles and in the Tully-Fisher relation, are reasonably well reproduced, as can be seen in Figures 3 and 4. It must be pointed out that the fact that the fitting procedure consists in minimizing $|\delta A|$ and ΔV does not necessarily imply that the distributions of points in the $A \times V_p$ diagram should follow the general trend given by equation (6); the points could be distributed in any possible way in that plane but amongst all of them, they do follow the behavior predicted from the observed Tully-Fisher relation.

5. DISCUSSION AND CONCLUSION

Presently, it is a very difficult task to deny the existence of extended dark material halos surrounding spiral galaxies, yet accepting them remains an uncomfortable position for many astronomers. The main reason for that is of course the fact that there is no *direct* observational evidence of such objects. They must be very dark, indeed.

Here, we have investigated the possibility of avoiding the dark halo hypothesis by means of a model which, in turn, suffers from a serious setback.

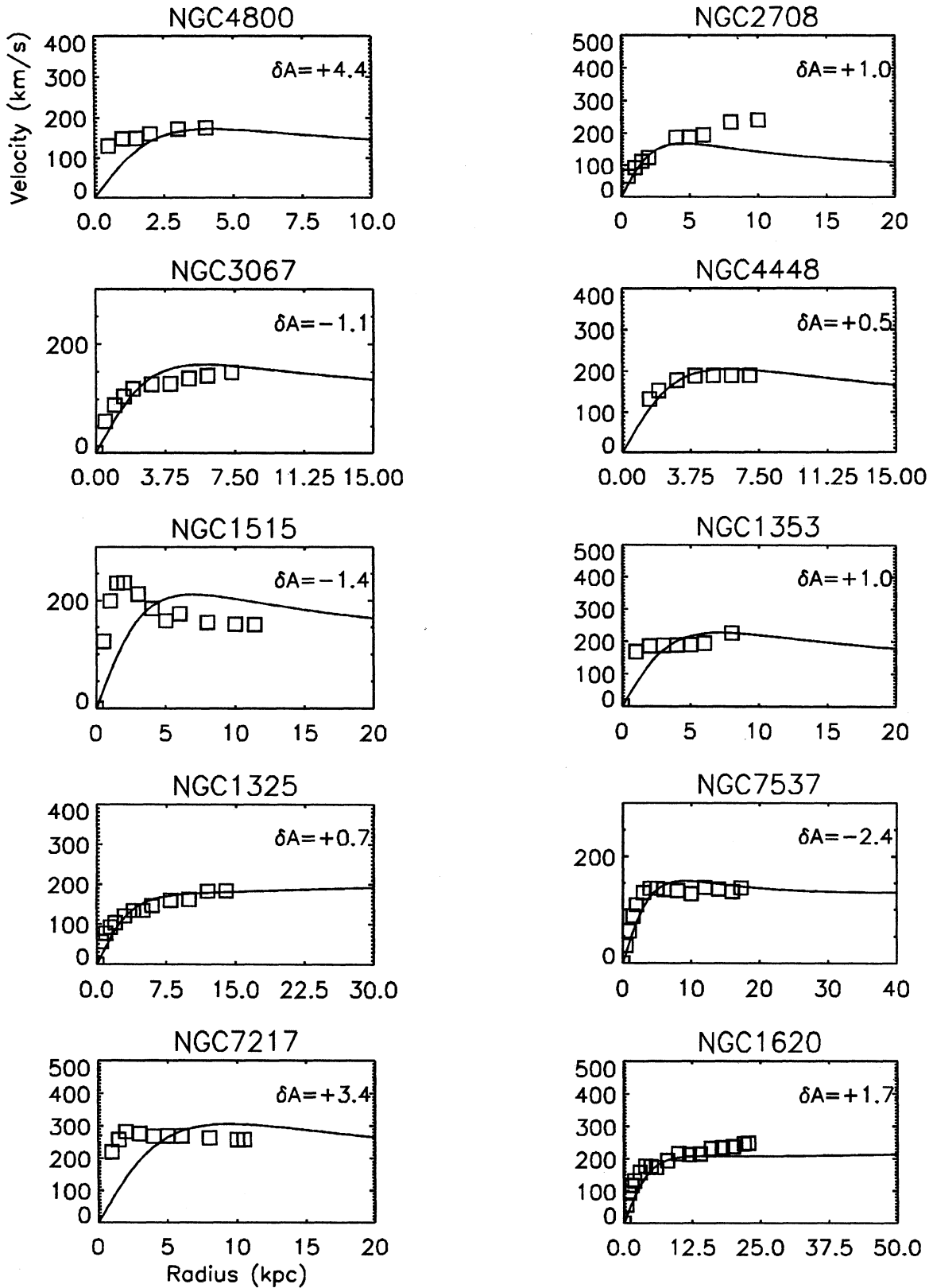


fig. 3. The squares represent the observations by Rubin et al. (1982), and the line is the AMOD fit to the rotation curve. The relative error in the AMOD index (δA) is given in each frame.

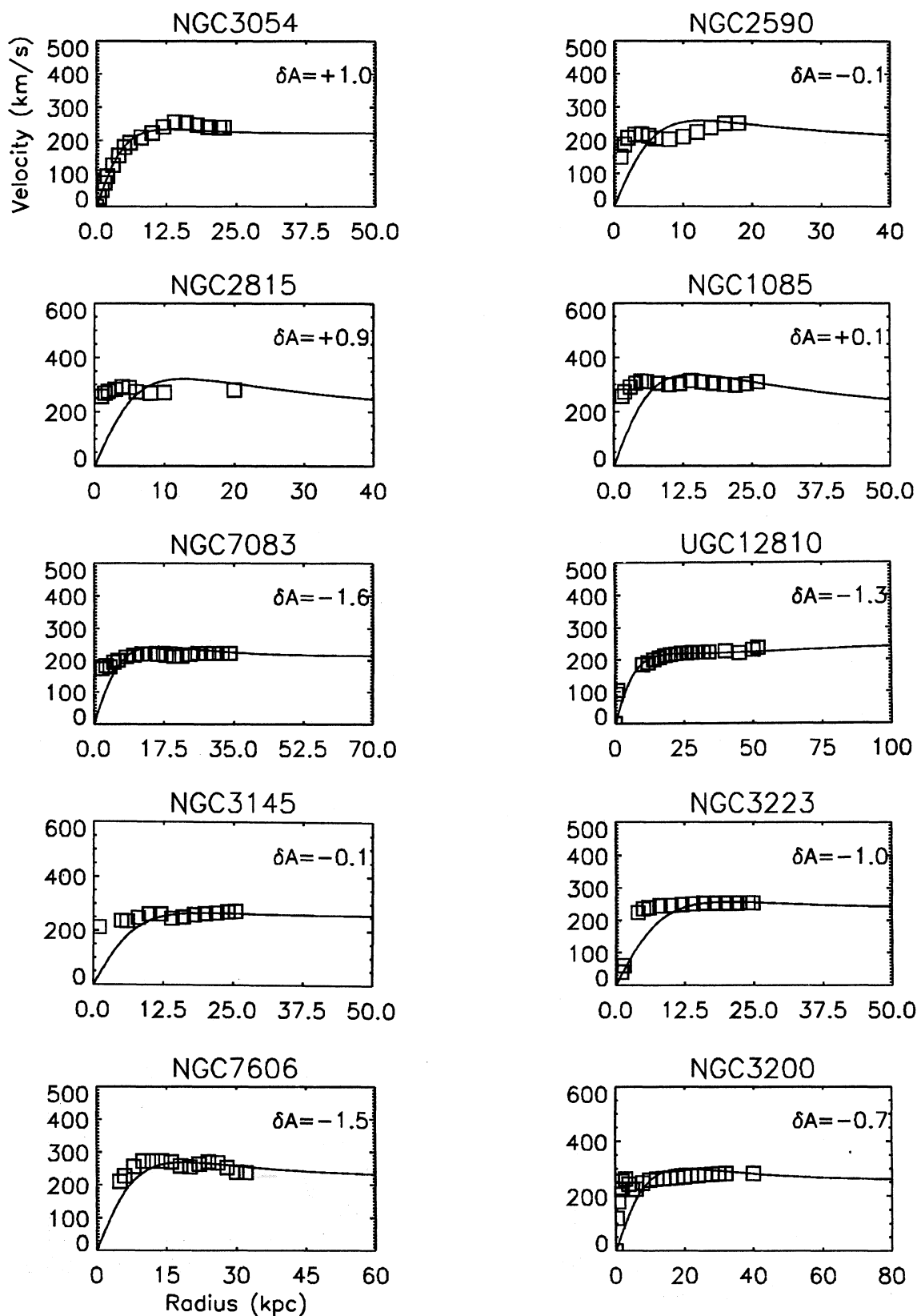


Fig. 3. (Continued).

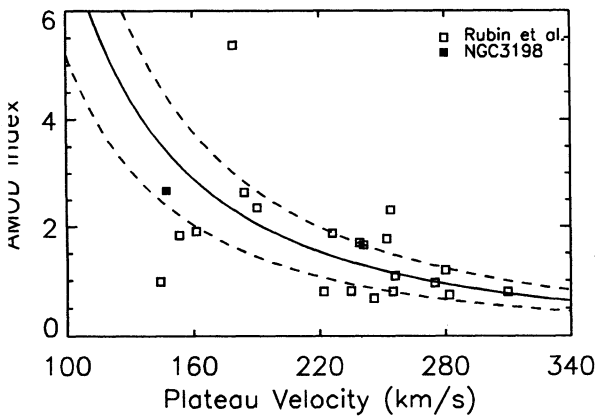


fig. 4. The solid line is given by equation (6), i.e., theully-Fisher relation in terms of the AMOD parameters A versus V_p . The dashed lines show the 30% error ar strip. The points were obtained from the fits to the station curves shown in Figure 3, and follow the general end given by the predicted curve.

TABLE 1

PARAMETERS AND AMOD INDICES
FOR SAMPLE GALAXIES

ame	V_p	R_{25}	r_o	$-\beta$	A	δA
(1)	(2)	(3)	(4)	(5)	(6)	(7)
3200	282.	46.0	140.0	0.90	0.74	-0.68
7606	246.	39.8	150.0	0.91	0.68	-1.48
3223	255.	34.8	120.0	0.92	0.80	-0.98
3145	275.	33.8	100.0	0.92	0.96	-0.07
12810	235.	51.4	110.0	0.95	0.81	-1.31
7083	222.	39.0	120.0	0.92	0.80	-1.56
1085	310.	34.8	260.0	0.84	0.80	+0.12
2815	280.	26.5	180.0	0.82	1.2	+0.85
2590	256.	39.6	100.0	0.88	1.1	-0.14
3054	239.	25.7	60.0	0.90	1.7	+1.03
11620	252.	29.8	55.0	0.92	1.8	+1.72
17217	254.	15.1	160.0	0.78	2.3	+3.37
17537	144.	18.3	90.0	0.94	0.98	-2.42
11325	184.	18.8	36.0	0.93	2.6	+0.69
11353	226.	14.0	140.0	0.84	1.9	+0.97
11515	153.	13.6	100.0	0.86	1.8	-1.40
14448	190.	11.0	120.0	0.84	2.4	+0.49
13067	161.	9.6	80.0	0.90	1.9	-1.11
12708	241.	14.7	120.0	0.86	1.7	+0.99
14800	179.	4.9	48.0	0.84	5.4	+4.41
13198	149.	17.1	36.0	0.92	2.7	-0.65

Notes: N3198 observed in H I by Begeman (1987), and the other galaxies in optical emission lines by Rubin et al. (1982). $H_0 = 50 \text{ km s}^{-1} \text{ Mpc}^{-1}$, and $M/L = 30$ for all galaxies. The plateau velocity, V_p , is given in km s^{-1} ; R_{25} and r_o in kpc.

the whole idea is based upon a drastic assumption in view of current standards, namely, it requires a spiral galaxy with an exceedingly high M/L (about 10–15 times as large as accepted values). On the other hand, and justifying such a speculation, there is no firm *direct* observational evidence supporting current M/L values of spiral galaxies.

A common feature of almost all model rotation curves, shown in Figure 3, is the badness of fitting in the small radius range. The AMOD potential is not able to give a detailed description of the rotational properties of spiral galaxies in the inner regions. The reason for that might be the oversimplified modeling of the hydrodynamical behavior of the gas component. Nevertheless, it gives a reasonable account of the global rotation of the gaseous medium as can be seen in the fitting of all of the sample rotation curves. It must be realized also that the Plummer sphere cannot represent details of the luminosity (mass) profiles of real galaxies, which has certainly contributed for some of the features shown in Figure 3.

The main point we want to make here is that disk rotation curves (either from gas emission lines or absorption from young stars) are not reliable to trace out the gravitational potential of a spiral galaxy as a whole. The toy model, discussed here and in Paper I, suggests that gas rotation may be indicating internal properties of the gaseous disk component rather than giving global information about the galaxy mass distribution.

AMOD can be tested observationally through a comparison between stellar and gas rotation curves in the inner regions of spiral galaxies. There, the effects caused by the gaseous character of the material are stronger than in the outer regions. That could be done from absorption line measurements, in the case of stellar rotation curves, and from emission line measurements from H II regions. Of course, the gravitational potential is the same for both gas and stars but the question is whether the *effective* galactic potential for gas is the same as for the stellar component. The physical processes acting on the gas component are certainly different from those on the stellar component. Special care must be taken when choosing the lines for the absorption measurements: one should look preferentially to old disk stars. Young OB stars preserve the kinematical characteristics of the gas medium where they were formed and are likely to give the same results for the rotation velocities as compared to the gas measurements.

Partial support from CNPq, Brazil — Process No. 300193/90-4) is gratefully acknowledged. I thank F.O. V\'eas Letelier for help in translating the abstract to Spanish.

REFERENCES

- Aaronson, M., Huchra, J., & Mould, J. 1979, *ApJ*, 229, 1
 Ashman, K.M. 1992, *PASP*, 104, 1109
 Assis, A.K.T. 1992, *Apeiron*, 13, 3
 Battaner, E., Garrido, J.L., Membrado, M., & Florido, E. 1992, *Nature*, 360, 624
 Begeman, K.G. 1987, Ph.D. Thesis, University of Groningen
 ———. 1989, *A&A*, 223, 47
 Broeils, A.H. 1992, Ph.D. Thesis, University of Groningen
 Faber, S.M., & Gallagher, J.S. 1979, *ARA&A*, 17, 135
 Freeman, K.C. 1970, *ApJ*, 160, 811
 González-Serrano, J.I., & Valentijn, E.A. 1991, *A&A*, 242, 334
 Larson, R.B., & Tinsley, B.M. 1978, *ApJ*, 219, 46
 Milgrom, M. 1983, *ApJ*, 270, 365
 ———. 1988, *ApJ*, 333, 689
 ———. 1991, *ApJ*, 367, 490
 North, J.D. 1965, *The Measure of the Universe, a History of Modern Cosmology*, (Oxford: Clarendon Press)
 Persic, M., & Salucci, P. 1993, *MNRAS*, 261, L21
 Rubin, V.C., Ford, W.K., Thonnard, N., & Burstein, D. 1982, *ApJ*, 261, 439
 Sanders, R.H. 1984, *A&A*, 136, L21
 ———. 1986, *A&A*, 154, 135
 ———. 1988, *MNRAS*, 235, 105
 ———. 1990, *A&AR*, 2, 1
 Schweizer, F. 1976, *ApJS*, 31, 313
 Schweizer, L.S. 1987, *ApJS*, 64, 427
 Soares, D.S.L. 1989, Ph.D. Thesis, University of Groningen
 ———. 1992, *RevMexAA*, 24, 3, (Paper I)
 Trimble, V. 1987, *ARA&A*, 25, 425
 Tully, R.B., & Fisher, J.R. 1977, *A&A*, 54, 661
 Valentijn, E.A. 1990, *Nature*, 346, 153
 van Albada, T.S., Bahcall, J.N., Begeman, K., & Sancisi, R. 1985, *ApJ*, 295, 305
 van Albada, T.S., & Sancisi, R. 1986, *Phil. Trans. R. Soc. London, A* 320, 447
 Whitmore, B.C., Rubin, V.C., & Ford, W.K. 1984, *ApJ*, 287, 66

Domingos S.L. Soares: Universidade Federal de Minas Gerais, Instituto de Ciências Exatas, Departamento de Física, Caixa Postal 702, 30161-970 Belo Horizonte, MG Brazil.